Mid-IR quantum cascade laser absorption CO concentration measurements of fuel-rich CH_4/O_2-mixtures doped with dimethyl ether and *n*-heptane behind reflected shock waves

Bo Shu, Jürgen Herzler, Oliver Welz, Mustapha Fikri*, Christof Schulz

IVG, Institute for Combustion and Gas Dynamics – Reactive Fluids,
University of Duisburg-Essen, 47048 Duisburg, Germany

Abstract

Exhaust gas from combustion under fuel-rich conditions can contain useful chemical compounds. Carbon monoxide (CO) is a main product during the partial oxidation or incomplete combustion of many hydrocarbons. Time-resolved CO concentrations during oxidation of fuel-rich mixtures of CH_4/dimethyl ether/O_2 and CH_4/*n*-heptane/O_2 (ϕ = 2) highly diluted in argon (96%) were measured behind reflected shock waves between 1400 and 2100 K at ~1 bar. Mid-IR quantum cascade laser absorption spectroscopy was employed as a high-sensitivity method for *in situ* time-resolved concentration measurement of CO using the P(20) rotational line of the fundamental (0-1) vibrational transition near 4.7 µm. Good agreement of the measured CO profiles and predictions of literature models was found.

Introduction

Flexibility between the conversion and storage of energy will be an important aspect in future energy systems, especially when considering the fluctuating availability of renewable energies. In times of low demand but high availability of energy, an interesting concept is the use of external mechanical or electrical energy in internal combustion engines (ICEs) to convert "cheap" chemicals (e.g., natural gas) into higher-value chemicals so that most of the exergy of the cheap fuels is stored. This production of chemicals typically proceeds at fuel-rich conditions, far away from current operating regimes of ICEs. A fundamental understanding of the chemical kinetics under these conditions and the availability of validated reaction mechanisms for these fuel-rich conditions are essential for the successful implementation of such processes. However, most of the reaction mechanisms published in the literature are validated preferentially for lean and stoichiometric mixtures, because these conditions are important in ICEs and gas turbines.

Time-resolved concentration measurements of combustion species such as NO [1], H_2O [2], CO_2 [3], and CO are valuable validation targets to test the predictions of these models. For these species, laser spectroscopy is well-suited because it is sensitive, non-intrusive and exhibits high time resolution [4].

In the context of partial oxidation (e.g., oxidation at fuel-rich conditions) for fuel conversion, we present high-temperature time-resolved CO-concentration measurements from fuel-rich mixtures of CH_4/dimethyl ether (DME)/O_2 and CH_4/*n*-heptane/O_2 (ϕ = 2) highly diluted in argon and helium (sum of the mole fractions of Ar and He of 96%) studied between 1400 and 2000 K at pressures of 1–2 bar behind reflected shock waves. Absorption measurements were performed with a mid-IR continuous wave quantum cascade laser (cw-QCL) (Alpes Lasers) with the central wavelength of 4.85 µm that accesses highly sensitive transitions [2] and thus enables accurate CO concentration measurements. The P(20) absorption line at 2059.91cm^{-1} was selected because it is strong and is not perturbed by neighboring lines of CO_2 and H_2O.

IR absorption of CO

The absorption coefficient (taken from the HITRAN database 2004 [5]) of CO in the wavelength range 1.5–5.5 µm at 1600 K is illustrated in Fig. 1. The fundamental band ($\Delta\nu$ = 1) near 4.6 µm has an absorption cross section that is larger compared to the first overtone band ($\Delta\nu$ = 2) near 2.3 µm and the second overtone band ($\Delta\nu$ = 3) near 1.55 µm [6-8] by two and four orders of magnitudes, respectively.

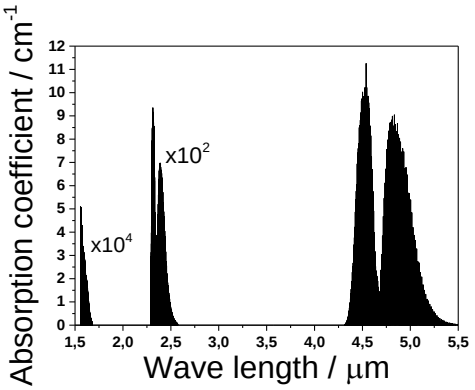

Fig. 1: Absorption coefficient of CO at 1600 K and 1 bar (from HITRAN 204 database [5]).

Following Beer Lambert's law, the ratio of transmitted (I_t) to incident light (I_0) through a probe volume with

* Corresponding author: mustapha.fikri@uni-due.de

a path length l containing the mole fraction x_i of a species i at a total pressure p is described by:

$$\left(\frac{I_t}{I_0}\right)_\upsilon = \exp(-Spx_i\phi_\upsilon l) \quad (1)$$

Here, S is the line strength of the transition at the frequency ν and ϕ_υ is the line shape function. Alternatively the relation can also be written as

$$\alpha_\upsilon = -ln\left(\frac{I_t}{I_0}\right)_\upsilon = Spx_i\phi_\upsilon l = k_\upsilon l\,, \quad (2)$$

where $\alpha_\upsilon$is the absorbance and k_υ the absorption coefficient.

The line strength is temperature dependent and is described typically relative to the line strength at the reference temperature T_0:

$$S(T) = S(T_0)\frac{Q(T_0)}{Q(T)}\left(\frac{T_0}{T}\right)exp\left[-\frac{hcE''}{k_B}\left(\frac{1}{T}-\frac{1}{T_0}\right)\right] \times\left[1-\exp\left(\frac{hc\upsilon_0}{k_BT}\right)\right]\left[1-\exp\left(\frac{hc\upsilon_0}{k_BT_0}\right)\right]^{-1} \quad (3)$$

Here, $Q(T)$ is the total partition function, E'' is the lower-state energy of the transition, υ_0 is the line center frequency and h, c, k_B are Planck's constant, speed of light and Boltzmann's constant, respectively.

The Voigt line shape function ϕ_υ describes the broadening characteristics of the line, which depends on temperature and pressure and is a convolution of Doppler and collisional broadening [9]. In HITRAN the broadening parameters are specified for air. Because in our mixtures the bath gas is a mixture of argon and helium instead of air, we use the temperature-dependent argon and helium broadening parameters for CO [10].

Experiment

Experiments on the oxidation of CH_4/DME/O_2 and CH_4/*n*-heptane/O_2 mixtures were performed in a shock tube with a length of driver and driven sections of 3 and 5.5 m, respectively [11], and an inner diameter of 8 cm. An aluminum diaphragm is used to separate the driver from the driven section. The driven section is equipped with four pressure transducers (PCB model 112A03), from which we obtained the shock velocity, which is used to calculate temperature and pressure behind the reflected shock using ideal shock relations (with an uncertainty in the temperature of ~1%). One additional transducer (Kistler 603A) is installed 20 mm upstream of the end wall. Two sapphire windows are also installed 20 mm upstream of the end wall for optical access. Test mixtures were prepared in a 50 l stainless-steel mixing tank and allowed to homogenize over night before use.

Progress of the oxidation reaction was followed by time-resolved laser-absorption measurements of CO. A schematic of the experimental arrangement is shown in Fig. 2. The cw-QCL laser used to probe absorption of CO is housed with thermoelectric cooling (TEC) elements and collimating optics in a sealed laser housing (HHL housing). The operating wavelength of the laser is tuned by varying the input temperature and current, which are controlled by a TEC controller (Alpes Laser TCU 200) through the integrated TEC element and current controller (ILX Lightwave LDX-3232), respectively.

Light emitted from the cw-QCL laser is focused into the center of the shock tube through a concave mirror and then collimated again by a second concave mirror with the same focal length that is placed symmetrically on the other side of shock tube. Afterwards, the laser beam passes through a beam-splitter (CaF_2) to reduce the laser power in order to avoid saturation of the detector. A band pass filter (4.855 µm ±88 nm) is installed in front of the detector (VIGO) to eliminate unwanted emission signal from shock heated gases. To make sure that the laser wavelength corresponds to the maximum of the CO absorption line, the laser light was guided through an 8 cm long well-sealed stainless-steel cell filled with a CO/Ar mixture at room temperature prior each shock-tube experiment.

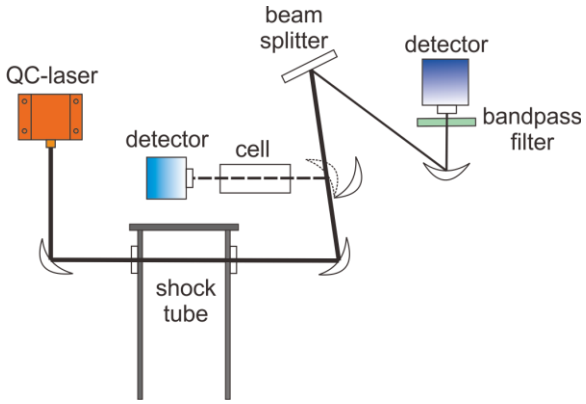

Fig. 2: Experimental arrangement for time-resolved CO measurement in a shock tube.

Spectral line characterization

With the current cw-QCL different lines are accessible in the mid-IR. The accessible frequency ranges between 2053 and 2062 cm^{-1} where the P(20) and P(14) transitions are located. Figure 3 shows a section of the spectrum between 2058 and 2062 cm^{-1} simulated with HITRAN for 1% CO, 10% H_2O and 1% CO_2 at 2000 K and 1 bar. Because the P(20) line is stronger than the P(14) line and is not perturbed by interfering absorption from species such as H_2O or CO_2, all measurements were carried out using the P(20) line.

Line strength for P(20)

We determined the temperature-dependent line strength of CO (eq. 2) using a mixture of 0.5% CO and 2% H_2 in Ar. H_2 was added to accelerate vibrational relaxation of CO. After shock heating the mixture, we found that establishment of thermal equilibrium in the vibrational degree of freedom in CO by energy transfer can take up to 1 ms under our conditions. In presence of

H_2 the relaxation time is however very short (50 µs).The mixtures were shock-heated in the temperature range from 1000 to 2500 K (T_5) at pressures of 1.0–1.6 bar (p_5). According to eq. 2, the absorption coefficient can be determined from the measured. Fig. 4 shows the measured absorbance during a typical shock tube experiment. At room temperature the absorbance is about 0.06 and increases to 0.5 behind the incident wave (p_2, T_2). The subsequent large spike is due to schlieren effects as a result of the passage of the reflected shock wave at the optical axis. Based on the known initial CO concentration and broadening factors, the line strength can be determined. Fig. 5 illustrates the measured line strengths of the P(20) transition from 1000–2500 K in comparison with calculated line strengths from the HITRAN database [5]. Measured and calculated values show an excellent agreement with a maximum deviation < 1.6%.

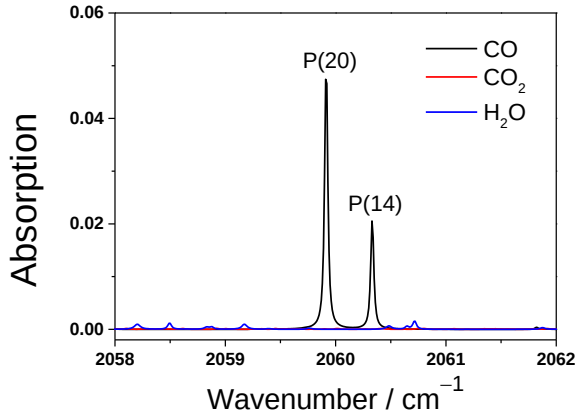

Fig. 3: Simulated spectra based on HITRAN of 0.1% CO, 1% CO_2, and 1% H_2O in air at T = 2000 K, p = 1 bar, l = 8 cm.

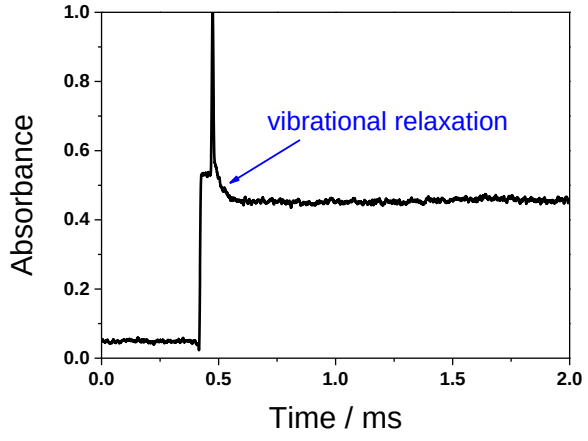

Fig. 4: Absorbance measurement based on fixed-wavelength direct laser absorption from a 0.5% CO/2% H_2/Ar mixture (T_5 = 1528 K, p_5 = 1.51 bar).

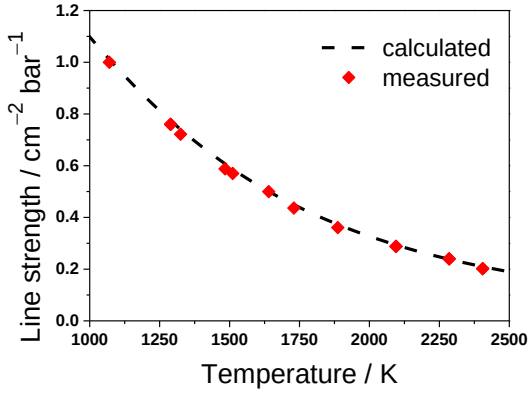

Fig. 5: Comparison of the measured line strength of the P(20) transition with the simulations based on the HITRAN database at temperatures of 1000–2500 K.

Results and discussion

CO measurement during CH_4/DME and CH_4/n-heptane oxidation

We applied time-resolved laser absorption measurements to probe CO formation from oxidation of fuel-rich mixtures of CH_4/DME/O_2 and CH_4/*n*-heptane/O_2 (ϕ = 2) highly diluted in argon/helium behind reflected shock waves. Mixtures of 1.9% CH_4, 0.1% DME and 2.05% O_2 diluted in 75.95% Ar and 20% He were investigated at temperatures between 1400 and 2100 K and pressures of 1.0–1.7 bar. Helium was added to accelerate vibrational relaxation of CO and was chosen instead of H_2 because it is inert and therefore does not participate in the oxidation [12]. 20% He was sufficient to minimize the influence of vibrational relaxation of CO on the absorption measurements (we observed evidence that CO is at least partly formed in vibrationally excited modes during oxidation). Fig. 6 shows a typical absorbance profile and the corresponding CO concentration history inferred from Eq. (2).

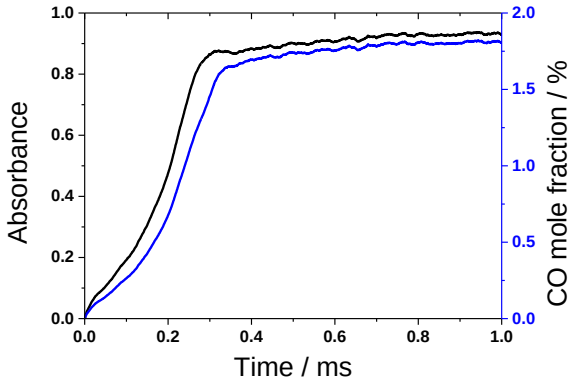

Fig. 6: CO absorbance during the oxidation of mixture of CH_4/DME/O_2 (1.9%/0.1%/2.05%) balanced in 75.95% argon and 20% helium at T_5 = 1777 K and p_5 = 1.35 bar. Black line: absorbance, blue line: CO mole fraction.

Because the oxidation is accompanied by a strong temperature increase (~400 K), it was necessary to account for the temperature dependence of the line strength when inferring the CO mole fraction. Because our experiment did not allow for *in situ* temperature measurements, we determined the temperature change using simulations based on the chemical kinetics model of Yasunaga et al. [13] under the constant-volume assumption and used this information to determine absolute CO concentrations. Additionally, the pressure change was taken into account to calculate the broadening parameters in the line shape function ϕ_v. Fig. 7 illustrates the simulated temperature and pressure changes under the constant-volume assumption.

Fig. 8 shows a comparison of measured CO concentration-time profiles with simulations using the models of Yasunaga et al.[13], Zhao et al. [14], and Burke et al. [15], respectively. We show only the experimental CO concentration obtained from the absorbance measurements using the *T* and *p* changes predicted by the model of Yasunaga et al. because the other two models predict very similar *T* and *p* changes, the determined CO concentrations are insensitive to the model chosen. The measured CO profiles agree well with the model of Yasunaga [13] for the plateau values although some discrepancies exist for the CO build-up at 1777 K, where the model predicts a somewhat delayed CO formation. The models of Zhao et al. and Burke et al. also predict the measured plateau value well and show a delayed but compared to the model of Yasunaga et al. slightly faster CO build-up. At higher temperature, all three models predict a slightly faster CO formation compared to our experimental results.

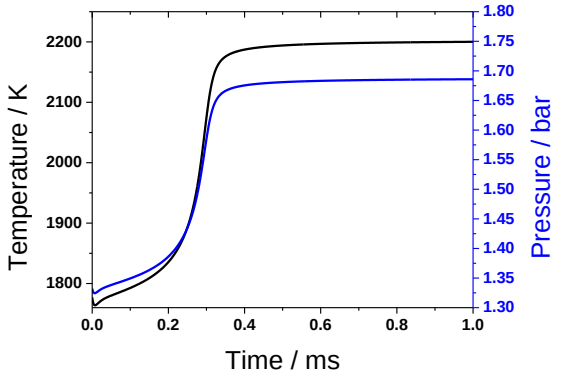

Fig. 7: Simulated temperature and pressure for an experiment with mixture of CH_4/DME/O_2 (1.9%/0.1%/2.05%) balanced in 75.95% argon and 20% helium at 1777 K and 1.35 bar.

Similar measurements were performed for mixtures containing 1.9% CH_4/0.1% *n*-heptane/2.45% O_2 balanced in Ar and 20% He. Oxidation was investigated at temperatures of 1600–2000 K and pressures of 1.0–1.6 bar. Here, changes in *T* and *p* during the reaction based on predictions from the mechanism of Mehl et al. [16] were taken into account to derive CO concentrations from the measured absorbance. The measured CO concentration time-histories are plotted in the Fig. 9 and compared to simulations based on the models of Mehl et al. [16] and Ranzi et al. [17] under the constant-volume assumption.

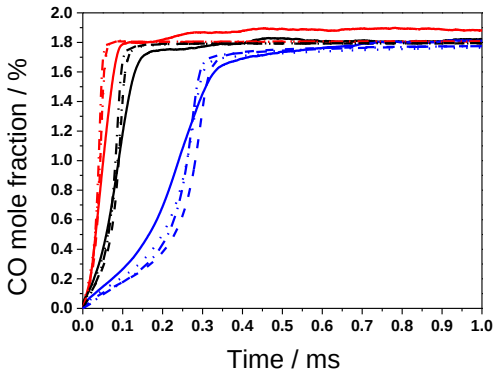

Fig. 8: CO measurements of a 1.9% CH_4/ 0.1% DME/ 2.05% O_2 / 20% He / Ar mixture behind the reflected shock waves at 2132 K (red), 1950 K (black), and 1777 K (blue), compared with simulations based on literature mechanisms. Full lines: measured CO time-histories, dotted lines: model of Zhao et al., [14] dashed lines: model of Yasunaga et al., [13] dashed dotted lines: model of Burke et al. [15].

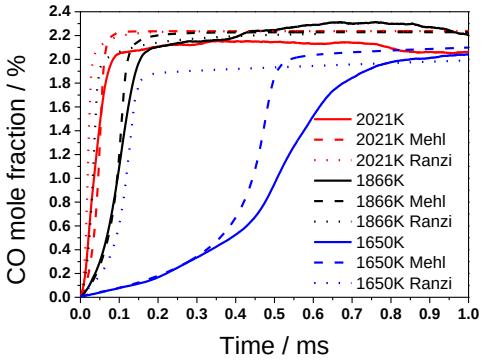

Fig. 9: CO measurements of a 1.9% CH_4/0.1% *n*-heptane/2.45% O_2/20% He/Ar mixture behind the reflected shock compared with simulations using the Mehl et al. mechanism [16] and Ranzi et al. mechanism [17].

The simulations based on the model of Mehl et al. [16] show good agreement with our measurements at 1866 K and 2021 K. At lower temperature (1650 K), the simulation predicts slightly faster CO formation than the measurement, but the prediction of the peak value of CO agrees well with the measurement. Simulations with the model of Ranzi et al. [17] predict a substantially faster CO formation compared to both measurement and simulation of Mehl et al. at all three conditions, but the prediction of the plateau value are similar to Mehl et al. and results from our measurements.

Conclusions

Quantum cascade laser mid-IR laser absorption spectroscopy was applied for time-resolved measurements of the formation of CO from partial oxidation of fuel-rich mixtures ($\phi = 2$) of CH_4 with DME (1.9% CH_4/0.1% DME/2.05% O_2/20% He/ Ar) and CH_4 with *n*-heptane (1.9% CH_4/0.1% *n*-heptane/ 2.45% O_2/20% He/Ar) at 1400–2100 and 1600–2000 K, respectively, behind reflected shock waves. CO is a major product at these conditions. In the laser absorption measurements, the P(20) transition of CO centered at 2059.91 cm^{-1} was selected and the temperature-dependent line-strength was determined between 1000–2500 K using a known CO/H_2/Ar mixture to infer absolute concentrations from the measured signals. H_2 was added to lower the vibrational relaxation time. Good agreement of the obtained values of the line strength with the literature was found.

For the partial oxidation experiments, the measured CO concentration time-histories were compared to predictions of the latest mechanisms of Yasunaga et al. [13], Zhao et al. [14], and Burke et al. [15] for CH_4/DME mixture, and Mehl et al. [16] and Ranzi et al. [17] for CH_4/*n*-heptane mixture. Good agreements were found with the models of Yasunaga et al., Zhao et al. and Burke et al. for CH_4/DME and Mehl et al. for CH_4/*n*-heptane mixtures.

Acknowledgment

Financial support of this work by the German Research Foundation within the framework of the DFG research unit FOR 1993 ‘Multi-functional conversion of chemical species and energy’ (GV2) is gratefully acknowledged.

References

1. C. Schulz, V. Sick, J. Wolfrum, V. Drewes, M. Zahn, R. Maly, Proc. Combust. Inst. 26 (1996) 2597-2604.
2. C. S. Godenstein, C. A. Almodovar, J. B. Jeffries, R. K. Hanson, Meas. Sci.Techno*l.* 25 (2014) 105104.
3. A. Farooq, J. B. Jeffries, R. K. Hanson, Appl. Phys. B 90 (2008) 619-628.
4. M. G. Allen, Meas. Sci.Technol. 9 (1998) 545-562.
5. Hitran, *http://www.cfa.harvard.edu/hitran*.
6. D. T. Cassidy, L. J. Bonnell, Appl. Opt. 27 (1988) 2688-2693.
7. R. K. Hanson, P. K. Falcone, Appl. Opt. 17 (1978) 2477-2480.
8. M. E. Webber, J. Wang, S. T. Sanders, D. S. Bear, R. K. Hanson, Proc. Combust. Inst. 28 (2000) 407-413.
9. R. K. Hanson, *Introduction to Spectroscopic Diagnostics for Gases*, standford university, 2001.
10. W. Ren, A. Farooq, D. F. Davidson, R. K. Hanson, Appl. Phys. B 107 (2012) 849-860.
11. M. Bozkurt, M. Fikri, C. Schulz, App. Phys. B 107 (2012) 515-527.
12. R. S. Tranter, B. R. Giri, J. H. Kiefer, Rev. Sci. Inst. 78 (2007) 34101-1-11.
13. K. Yasunaga, F. Gillespie, J. M. Simmie, H. J. Curran, Y. Kuraguchi, H. Hoshikawa, M. Yamane, Y. Hidaka, J. Phys. Chem. A 114 (2010) 9098-9109.
14. Z. Zhao, M. Chaos, A. Kazakov, F. L. Dryer, Int. J. Chem. Kinet. 40 (2008) 1-18.
15. U. Burke, K. P. Somers, P. O’Toole, C. M. Zinner, N. Marquet, G. Bourque, E. L. Petersen, W. K. Metcalfe, Z. Serinyel, H. J. Curran, Comb. Flame 162 (2015) 315-330.
16. M. Mehl, W. J. Pitz, C. K. Westbrook, H. J. Curran, Proc. Combust. Inst. 33 (2011) 193-200.
17. E. Ranzi, A. Frassoldati, R. Grana, A. Cuoci, T. Faravelle, A. P. Kelley, C. K. Law, Progr. Energy Combust. Sci. 38 (2012) 468-501.